arXiv:0704.2637v1 [astro-ph] 20 Apr 2007

Observational consequences of the hypothesized helium rich stellar population in ω Centauri.

G. Newsham and D. M. Terndrup

Department of Astronomy, The Ohio State University, Columbus, OH 43210-1173

`newshamg@astronomy.ohio-state.edu,terndrup@astronomy.ohio-state.edu`

ABSTRACT

In response to the proposed high helium content stars as an explanation for the double main sequence observed in ω Centauri, we investigated the consequences of such stars elsewhere on the color-magnitude diagram. We concentrated on the horizontal branch where the effects of high helium are expected to show themselves more clearly. In the process, we developed a procedure for comparing the mass loss suffered by differing stellar populations in a physically motivated manner. High helium stars in the numbers proposed seem absent from the horizontal branch of ω Centauri unless their mass loss history is very different from that of the majority metal-poor stars. It is possible to generate a double main sequence with existing ω Centauri stars via accretion of helium rich pollution consistent with the latest AGB ejecta theoretical yields, and such polluted stars are consistent with the observed HB morphology of ω Centauri. Polluted models are consistent with observed merging of the main sequences as opposed to our models of helium rich stars. Using the $(B-R)/(B+V+R)$ statistic, we find that the high helium bMS stars require an age difference compared to the rMS stars that is too great, whereas the pollution scenario stars have no such conflict for inferred ω Centauri mass losses.

Subject headings: globular clusters: general — globular clusters: individual (ω Centauri)

1. Introduction

The globular cluster ω Centauri has long been known to exhibit a wide range of metallicities (e.g., Dickens & Wooley 1967; Freeman & Rodgers 1975; Suntzeff & Kraft 1996), possibly in discrete subpopulations. Norris et al. (1996) presented an extensive survey of

Ca-triplet abundances, revealing a majority metal-poor component at [Ca/H] $= -1.4$, an intermediate metal-poor peak at [Ca/H] $= -0.9$, and a long tail extending up to a [Ca/H] $= -0.3$. Pancino et al. (2000) discussed wide-field BI photometry and the Norris et al. abundances, identifying four peaks at [Ca/H] $= -1.4$, -1.0, -0.5 and -0.1. The [Ca/Fe] ratio is almost flat as a function of [Fe/H] (Norris & Da Costa 1995) with an average value $\langle$[Ca/Fe]$\rangle \approx +0.4$, so the first two peaks of the abundance distribution have [Fe/H] ≈ -1.7 and -1.3, respectively.

The peculiarities of ω Centauri were further revealed by the discovery of multiple turn-offs and a double main sequence (MS) in HST photometry by Bedin et al. (2004). As seen in their Figure 1, the two main sequences are clearly separated by $\Delta(V-I) \sim 0.06$ over several magnitudes in V, with the region between them almost devoid of stars. It can be seen that towards faint magnitudes the two main sequences merge together, this is even more obvious in the latest data of Villanova et al. (2007). The blue main sequence (bMS) is less populated than the red main sequence (rMS), comprising about 25% to 35% of MS stars. As discussed in Bedin et al. (2004), if metallicity alone were controlling the morphology of the main sequence, the MS would be about 0.03 magnitude in width with a concentration toward the blue edge corresponding to the [Fe/H] $= -1.7$ majority ($\approx 65\%$) population, a tail towards the red of stars corresponding to the intermediate metallicity population ($\approx 30\%$) and a small ($\approx 5\%$) of the stars redder still.

Of the various hypotheses put forth in Bedin et al. (2004) to explain the double main sequence, most intriguing has been the idea that the bMS stars have an unusually high helium content. Norris (2004) noted that the rMS and bMS stars were present in a ratio of 2:1, which was approximately like the ratio of stars with [Fe/H] $= -1.7$ to those near [Fe/H] $= -1.3$. Taking the Revised Yale Isochrones (Green et al. 1987) and fitting them to a synthetic color magnitude diagram (CMD) of ω Centauri, Norris found that the double main sequence can be reproduced if the intermediate metallicity population is more helium rich by $\Delta Y \approx 0.10 - 0.15$ than the metal-poor population.

Piotto et al. (2005) undertook a spectroscopic investigation of the bMS and rMS stars in ω Centauri. They obtained VLT spectra of 17 rMS stars and 17 bMS stars which were combined respectively to form a single rMS and single bMS composite spectrum. They found that the rMS stars have [Fe/H] $= -1.57$ and the bMS stars have [Fe/H] $= -1.26$, close to the largest two peaks in the distribution of abundances on the giant branch. Piotto et al. (2005) also fit new stellar isochrones to the bMS and showed that it can best be modelled with $0.35 \lesssim \mathrm{Y} \lesssim 0.45$, the best value being $Y = 0.38$. This confirms the Norris (2004) result but with metallicities directly from the MS and more up-to-date stellar models. Similar conclusions were drawn by Lee et al. (2005), who determined a best fit to the observations implied a bMS helium content of 0.38, implying $\Delta Y \approx 0.15$. D'Antona et al. (2005) have reached a similar conclusion of a spread of helium content for the main sequence stars of NGC 2808 using HST photometry. They noted that the color distribution is not Gaussian and is wider than that expected for a single metallicity population. They found some 20% of the stars are much bluer than expected and from their stellar models conclude that the helium mass fraction of these stars is $Y \sim 0.4$.

Attempts to explain the high helium content of the bMS stars have not been entirely successful. If massive stars in the metal-poor population were responsible for both the helium and metal enrichment of the intermediate metallicity stars, values of $\Delta Y/\Delta Z \sim 100$ are implied (e.g., Norris 2004), far in excess of the canonical value $3-4$ (e.g., Pagel 1992). Piotto et al. (2005) noted that massive stars should also produce a large amount of carbon, nitrogen, and oxygen, but in ω Centauri the total $[(\mathrm{C+N+O})/\mathrm{Fe}]$ abundances for all stars is about $+0.4$ dex (Norris & Da Costa 1995). This is also the case for enrichment by AGB star winds (Karakas et al. 2006). Bekki & Norris (2006) extensively discussed enrichment by intermediate mass AGB stars, massive stars that produce helium-rich winds (see Maeder & Meynet 2006) and SNe II. They concluded that for reasonable Initial Mass Function (IMF) choices ω Centauri could not have survived disintegration due to cluster mass loss. The most serious problem with the AGB scenario is that the total mass of ejecta from rMS AGB stars is too small to be consistent with the observed fraction of the bMS of ω Centauri. If ω Centauri formed with a very unusual IMF, producing little or no SNe II, then the observed bMS fraction can be reproduced; that is, however, inconsistent with the known presence of neutron stars in ω Centauri. Similarly, the number of massive stars with helium-rich winds do not contribute a large enough mass fraction of ejecta for allowable IMF choices. In addition, there would be little difference in metallicity between the rMS stars and the massive star wind ejecta, which is at odds with the Piotto et al. (2005) result on the metallicity difference between the bMS and rMS populations. Conversely, the problem with the SNe II scenario is that the heavy element abundances would be too high to be consistent with the bMS stars forming from SNe II ejecta. The conclusion was that neither alone or combined could these three sources explain the bMS stars as being formed exclusively from the ejecta of rMS stars. Recent work by Choi & Yi (2007) have concluded the only way to achieve such high helium enrichments without a commensurate level of metal production is by appealing to Population III star ejecta as the source of the material that formed the bMS. However, they admit this scenario is itself of an extreme nature.

Several studies have tried to find the evolutionary descendants of the He-rich population on the horizontal branch (HB). Stars with high ($Y \gtrsim 0.35$) helium content would reach the tip of the RHB (TRGB) with a reduced mass since they have shorter lifetimes. This would make the HB both hotter (bluer) and more luminous when compared to stars of lesser helium content (D'Antona et al. 2002). D'Cruz et al. (2000) & Momany et al. (2004) noted that ω Centauri does have a noticeably blue HB with substantial numbers of Extreme Horizontal Branch (EHB) stars with an effective temperature ($T_{\rm eff}$) greater than 20,000K. This has been noted as qualitative evidence of the bMS stars progeny populating the HB of ω Centauri (Norris 2004; Piotto et al. 2005; Lee et al. 2005).

Recent observations of the RR Lyrae variables in ω Centauri by Sollima et al. (2006) showed spectroscopically the presence of both metal-poor and intermediate metallicity stars in their sample of 74 RR Lyrae variables. These intermediate metallicity variables are not consistent with a high helium enhancement, in that they do not have a higher luminosity and they have an ordinary relationship between period and luminosity. Thus, at least some intermediate metallicity stars have normal helium abundances. As Sollima et al. (2006) themselves noted, this is not necessary a strong argument against the enhanced helium hypothesis, since bMS stars would not appear in the RR Lyrae instability strip unless they are some 4 Gyr younger than the rMS population or have undergone a radically different mass loss history.

In this paper we perform a quantitative calculation of the color distribution of HB stars for various helium abundances. We also investigate whether accretion of helium-rich material onto existing stars can produce the observed double main sequence, and follow the evolution of these stars to the HB. A description of the stellar evolutionary calculations we performed is presented in §2, which also discusses models of stars with homogeneous high helium abundance. Models with a high surface abundance of helium are presented in §3. In §4 we summarize our results.

2. Models with homogeneous enhanced helium

2.1. Stellar Evolution Models

We computed evolutionary tracks appropriate for ω Centauri using the modern version (Sills et al. 2000) of the Yale Rotating Stellar Evolution Code (YREC, Guenther et al. 1992); in the computations, the rotation routines were turned off. Nuclear reaction rates are taken from Gruzinov & Bahcall (1998) and the heavy element mixture is that of Grevesse & Noels (1993). Gravitational settling of helium and heavy elements is included in these models, as in Bahcall & Loeb (1990) and Thoul et al. (1994). We also include neutrino losses from photo, pair, bremmstrahlung and plasma neutrinos, following Itoh et al. (1996).

We use the OPAL opacities (Iglesias & Rogers 1996) for temperatures $\log T \geq 4$. For lower temperatures, we employ the molecular opacities of Alexander & Ferguson (1994). The alpha-enhanced low T opacities are known to be in error (Weiss et al. 2006) but this does not affect our calculations as we used the solar mixture opacities. For regions of the star with $\log T \geq 3.7$, we use the 2001 version of the OPAL equation of state (Rogers et al. 1996)[1] and for $\log T < 3.7$ we take the equation of state from Saumon et al. (1995).

For the surface boundary conditions, we use the stellar atmosphere models of Allard & Hauschildt (1995), which include molecular effects and are therefore appropriate for low mass stars. We use the standard Böhm-Vitense mixing length theory (Böhm-Vitense 1958; Cox et al. 1968) with $\alpha = 2.013$, obtained by calibrating a solar model against observations of the solar radius (6.9598×10^{10} cm) and luminosity (3.8515×10^{33} erg s^{-1}) at the present age (4.57 Gyr) and metal fraction ($Z = 0.01757$) of the Sun. By comparison, models of the Sun excluding diffusion require $\alpha \approx 1.7$ (e.g., Pinsonneault et al. 2003).

The helium content of "ordinary" (i.e., not enhanced in helium) ω Centauri stars was computed using the primordial helium abundance abundance $Y_p = 0.23$ and the enrichment parameter $\Delta Y/\Delta Z = 2.0$, in line with the treatment in the Yale-Yonsei isochrones of Yi & Demarque (2003). The value for Y_p is within, but on the low end of, the range of current estimates (e.g., Bono et al. 2002; Thuan & Izotov 2002; Olive & Skillman 2004, and references therein) although some values are considerably higher (e.g., Fukugita & Kawasaki 2006). This would yield a helium abundance for the Sun of $Y = 0.265$ in models lacking diffusion. Models compatible with helioseismology which include both rotational mixing and diffusion have a surface abundances $Y_{\odot,\mathrm{surf}} = 0.249 \pm 0.003$ and an initial solar composition $Y_\odot = 0.274$, $Z_\odot = 0.019$ (Bahcall et al. 2001). Such values would imply $\Delta Y/\Delta Z = 2.3$, close to $\Delta Y/\Delta Z = 2.1 \pm 0.4$ inferred for nearby field stars (Jimenez et al. 2003), but larger than $\Delta Y/\Delta Z = 1.3 \pm 0.2$ from open clusters in the solar neighborhood (An et al. 2007). At the low metallicities of the stars in ω Centauri, however, the properties of the models for unenhanced stars are insensitive to the exact value of the helium enrichment parameter.

All models began with a zero-age main sequence (ZAMS) model evolved from the deuterium-burning birthline. The ZAMS was defined as the point at which the core hydrogen abundance had dropped by 2% from the initial value. Horizontal branch models were created by rescaling the core masses, metallicity and envelope masses of horizontal branch models created for the YREC code provided by A. Sills (private communication). The core masses were determined from the corresponding RGB tip (TRGB) core masses from our evolved models and Zero Age Horizontal Branch (ZAHB) sequences developed by rescaling the envelope masses to define the ZAHB. This method of creating ZAHB sequences has been found to be adequate by Serenelli & Weiss (2005) with deviations at the few percent level being found for the hottest HB stars when compared to ZAHB models calculated directly through the core helium flash.

---

[1] Web updates at http://www-phys.llnl.gov/Research/OPAL/Download

We calculated theoretical isochrones by interpolating the model evolutionary tracks using a scheme based upon the algorithm of Bergbusch & Vandenberg (1992). The tracks, all with ages above 7 Gyr, have a simple topology, so we used five major evolutionary points to create the isochrones. These were the zero age main sequence point, the point of the exhaustion of core hydrogen, the base of the red giant branch, the red giant bump and the tip of the red giant branch (i.e., at the helium flash). Observational colors and magnitudes were calculated from $M_{\rm bol}$, log g and $T_{\rm eff}$ using the transformations of Vandenberg & Clem (2003).

2.2. Model populations

Norris (2004) and Lee et al. (2005) both modelled the bMS of ω Centauri as a population with [M/H] $= -1.27$ and a helium enhancement of $\Delta Y = 0.12 - 0.18$ over the rMS. Norris (2004) associated the bMS population with the second most common RGB metallicity, while Lee et al. (2005) used the the bMS metallicity as determined spectroscopically in Piotto et al. (2005).

In this present work we created isochrones for the two main sequence populations using parameters shown in Table 1, where we list the metal content, helium content, metallicity, the TRGB total mass, and the TRGB helium core mass. Here we are using models for the bMS that are homogeneous in helium content; below we compute models in which the outer convective zones are polluted with helium-rich material. Hereafter, the proposed helium-rich population in all evolutionary states shall be referred to as the bMS population, while the majority metal-poor stars shall be called the rMS population. We later discuss polluted models where we refer to a population with the metallicity of the bMS stars but with a normal helium content; we shall call this the intermediate metal poor population (MintP). Its characteristics are also shown in Table 1.

In Figure 1 we show isochrones for the bMS and rMS populations in the $M_V, B-V$ plane; both groups have an age of 13 Gyr. The two populations overlap at the turnoff (TO) but separate again high on the RGB, where the bMS stars now appear on the cool side of the rMS giant branch. As expected from theory, the ZAHB of the bMS is more luminous (by ~ 0.8 magnitudes) than that of the rMS. Both sequences merge on the hot tail of the blue HB.

2.3. Mass loss methods

In order to populate the ZAHB sequences we need to parameterize the mass loss at the TRGB. There are two approaches that are used to calculate a distribution of HB masses. In the first, mass loss is parameterized with mean value (ΔM) and a dispersion σ_M; the form of the mass loss distribution is often taken as a Gaussian. Using this approach, Lee et al. (1994) and Catelan (2000) studied the HB color distribution of several globular clusters, and found mean HB masses of $0.63 - 0.75 M_\odot$, implying mass losses of the order $0.1 - 0.2 M_\odot$. The presence of extremely blue HB stars in some clusters implies even greater mass losses, of the order $0.3 M_\odot$ (cf. Table 1), since these stars have a very thin ($M \leq 0.002 M_\odot$) hydrogen envelope surrounding the helium core.

Alternatively, some authors calculate mass loss during the RGB evolution, employing various empirical approximations. The mass loss scales with one or more physical parameters of the RGB star (see Catelan 2000, for a summary). It has long been questioned whether or not these formulae accurately estimate the mass loss rates of RGB stars. Origlia et al. (2002) showed that the observed loss rates are at least an order of magnitude greater than the predictions of the empirical formulae, and the rates do not seem to follow the dependence on luminosity, gravity, radius, or metallicity which appear in the empirical expressions. They also concluded that the mass loss occurs only in the last 10^6 years of RGB evolution (i.e., very near the TRGB) and is episodic in nature; the observed time scale for mass loss is greater than a few decades and less than a million years.

In this paper, we follow the first approach. The models are run to the TRGB with no mass loss. At the helium flash, we generate a distribution of HB masses to populate the ZAHB. By doing so, we do not need to follow the effect of mass loss on the structural evolution of stars near the TRGB.

Because the rMS and bMS stars reach the TRGB with quite different masses (Table 1), they may have a different average mass loss. Simply assuming a mean mass loss of order $0.2 M_\odot$ for the bMS would remove the entire envelope and part of the helium core, yet we know from EHB star spectra that hydrogen is present in these stars. We note that any mass loss greater than $0.174 M_\odot$ for the bMS stars at an age of 13 Gyr removes the entire hydrogen envelope of the star.

We consider several cases for computing the mass loss for bMS stars. The first case (Case I) corresponds to the situation in which the mass loss takes place on time scales shorter than the Kelvin-Helmholtz time, perhaps as short as the bottom of the range of time scales discussed by Origlia et al. (2002). Whatever the mechanisms operate to produce the mass loss, they have to remove material from the star by doing work against the gravitational potential. In Figure 2 we plot the acceleration of gravity at an interior point against ΔM; the latter is the total stellar mass minus the mass at the interior point. Shown are TRGB models of the bMS and rMS populations at an age of 13 Gyr. The bMS model is distinctly more compact in structure than the rMS star. Rapid mass loss, therefore, is likely to remove a smaller amount of material in helium-rich stars.

The second case (Case II) assumes that the time scale for mass loss is long, and that both populations have the same dependence of loss rate on luminosity. This implies that the total mass loss for the rMS and bMS stars would be in proportion to their evolutionary timescales near the TRGB. The bMS stars evolve more rapidly than the rMS stars, so in this case they would also have a lower amount of material removed, though more than in Case I.

We also compute (Case III) mass loss using an empirical mass loss law, the Reimers prescription as generalized in Catelan (2000). Such a prescription assumes that the mass loss rate includes a dependence on the luminosity, temperature and gravity of the star and that it occurs over a large timescale. Thus the total mass loss can be approximated as the product of the evolutionary timescale of the star on the upper RGB and the mass loss rate from the Reimers formula. In this case the mass loss is approximately the same in both rMS and bMS stars.

In Table 2, we show various ΔM for for rMS stars and the corresponding cases for mass loss of bMS stars. The lowest relative mass loss is for Case I, while the highest is for Case III. In the discussion following we calculate HB models using Case I. We justify this choice on the basis that it represents the most conservative case of mass loss, the other cases would push the HB stars from the bMS population to even higher temperatures producing even more of a clump in the HB tail that is not seen. We also feel that in light of the observational data of Origlia et al. (2002) that Case I is the physically most likely choice for mass loss. We implemented the mass loss by assuming a ΔM with a small dispersion, σ_M, to be subtracted from the TRGB mass for rMS stars. We found the mass of the immediate ZAHB star progenitor from the mass of the star at the TRGB on the appropriate isochrone. We took the ΔM value and found the local acceleration due to gravity, g, in the corresponding rMS TRGB stellar model. We then applied these values of g to the bMS model and calculated the corresponding ΔM and σ_M for the bMS model. The resulting ZAHB population distributions were proportioned in accordance to the observed numbers of rMS and bMS stars, with 70% from the rMS and 30% from the bMS.

2.4. Results

Figure 3 displays an example of the relative locations of the bMS and rMS stars on the HB. The plot is in the observational $(M_V, B-V)$ plane. The rMS population is shown as open triangles, and the bMS population as filled circles. The isochrones are also shown as solid and dashed lines, respectively. Here, both populations have an age of 13 Gyr. The ZAHB is populated with $\Delta M = 0.24 M_\odot$ and a dispersion of $\sigma_M = 0.015 M_\odot$ for the rMS stars and the equivalent $\Delta M = 0.143 M_\odot$ with a dispersion of $\sigma_M = 0.009 M_\odot$ for the bMS stars. The ZAHB populations stay on the hot tails of both ZAHB sequences, although the rMS population resides to the cooler side and is redder by about 0.15 magnitudes in $B-V$ and brighter on average by some 2 magnitudes in V.

In Figure 4 we see the effect of varying the mass loss prescription with $\Delta M = 0.20$ and $0.28 M_\odot$ for the rMS stars and equivalent ΔM of 0.118 and 0.168 $M_\odot$ for the bMS stars of 13 Gyr age. The stars are seen to remain on the hot tail of the ZAHB sequence with $B-V \lesssim -0.05$. For the rMS population, stars of the lowest 0.20 $\mathrm{M}_\odot$ mean mass loss start to appear on the horizontal region of the ZAHB extending all the way up to $B-V \sim 0.2$.

The effect of age on the ZAHB distribution is also shown in Figure 4 for the bMS stars at 7 Gyr age ($\Delta M = 0.143$ $\mathrm{M}_\odot$). This shows we can populate the ZAHB from the hot tail at $B-V \lesssim -0.1$ at 13 Gyr all the way to $B-V = 0.6$ at the extreme red end for a 7 Gyr bMS population. To clearly differentiate a high helium bMS population we should look for a more luminous stellar population at $B-V \gtrsim 0.0$ where the bMS stars populate a ZAHB some 0.8 magnitudes brighter. This effect is likely to result for bMS populations 2 to 6 Gyr younger than the rMS population with greater mass losses requiring a corresponding greater age difference. For bMS and rMS populations at the same 13 Gyr age the differences on the ZAHB is primarily one of color alone and the rMS stars being on average about 0.1 magnitudes in $B-V$ redder than the bMS ZAHB stars, though for equivalent mass losses the rMS stars are about $1-2$ magnitudes brighter in V.

2.5. Comparison with observations

In Figure 5, we plot the CMD of ω Centauri ground-based data of Rey et al. (2004). Also shown are the 13 Gyr isochrones and ZAHBs of the bMS and rMS populations from Figure 1. We followed Rey et al. in adopting $E(B-V) = 0.12$ and $(m-M)_V = 14.1$. Figure 6 shows the HB only along with the location of the RR Lyrae instability strip from Bono et al. (1995).

On the CMD, the majority of the HB stars lie within $14.4 < V < 16.4$ and $0.00 <$

$B-V < 0.32$. Following Norris (2004), we make the assumption these are mainly from the rMS population. If the age of the rMS population is 13 Gyr, then the rMS stars have lost a mass of $0.168 - 0.247 M_\odot$. For a Case I mass loss, the bMS stars at 13 Gyr would have lost $0.102 - 0.147 M_\odot$. This corresponds approximately to the location of the filled circles on Figure 4, so we should see the bMS stars between $-0.2 \leq B-V \leq -0.15$ and on average about $1.5 - 3.0$ mag fainter in V than the main HB. This would place them on the blue tail of the helium-rich HB, with $16.5 \leq V \leq 18.5$. For mass loss amounts described by Case II or III, the bMS stars would be even bluer and fainter forming a distinct clump at the bottom of the HB tail. Although there are many such stars on the CMD (Fig. 5) they are not present as expected from the relative numbers on the main sequence (Norris (2004) reached a similar conclusion) in which the bMS composes about 37% of the bMS plus rMS total (e.g., Ferraro et al. 2004; Sollima et al. 2007; Villanova et al. 2007).

We also checked the deeper ω Centauri HST CMD of Ferraro et al. (2004) using data furnished by A. Sollima (private communication). In analyzing the HST data we find that the EHB stars compose some $25\%\pm3\%$ of the HB population due to the bMS and rMS stars. This should be contrasted with the $37\%\pm2\%$ derived in the latest MS data by Villanova et al. (2007). The 10% of stars of higher metallicity that are not attributed to the bMS and rMS populations would not appear in the main clump of the HB for the inferred rMS mass loss as determined from our theoretical models discussed above so we counted from the main clump and blueward giving us the rMS and bMS stars only. Note that since the HB lifetime for both rMS and bMS stars is similar, as expected from theory and confirmed in our models, then this difference in the number of bMS to rMS HB stars is not due to the effects of a different HB evolutionary lifetime. Even if *all* the stars in the blue tail of the HB are in the bMS population, they number only about 25% of the stars on the main part of the HB.

It does not help to assume that the bMS stars are younger than 13 Gyr, and so have redder colors. If the bMS population is 2 Gyr younger, our models predict that they would be found on the ZAHB with colors $0.05 < B-V < 0.16$ and brighter than the rMS HB by 0.8 magnitudes in V. When we count the stars in this region of the CMD, we find that they number $\sim 1.3\%$ of the number of stars main clump on the HB. Some of these stars in this region of the CMD are undoubtedly rMS stars that have evolved off the ZAHB, thus reducing the number of possible bMS stars in that region. It thus appears that we do not see the substantial number of stars in the CMD at the location we would expect the bMS stars to appear. These calculations are also consistent with the conclusions of Sollima et al. (2006), who failed to find any RR Lyrae stars in ω Centauri that were helium rich, as indicated by a high luminosity. Such stars would be in the instability strip only if they were $2 - 5$ Gyr younger than the rMS population. Such young ages are excluded by the analysis of the turnoff region (Sollima et al. 2005; Lee et al. 2005).

Using the Rey et al. CMD, we also calculated the $(B - R)/(B + V + R)$ statistic (Lee et al. 1994), where B, V and R are the numbers of red HB (RHB), RR Lyrae variables and blue HB (BHB) stars respectively. Following Rey et al. (2004), we define the RHB stars as having $14.2 < V < 14.85$ and $0.55 < B-V < 0.71$. In total we find 2781 HB stars in the ω Centauri CMD of which 2497 are BHB stars, 149 in the RR Lyrae instability strip, and 135 are RHB stars. This gives us $(B - R)/(B + V + R) = 0.85 \pm 0.01$, with the error arising from counting statistics. We shall use this result later as a discriminator in discussing polluted stellar models versus homogeneous helium-rich bMS stars. Using the HST data of Ferraro et al. (2004) we calculated $(B - R)/(B + V + R) = 0.85 \pm 0.01$ which is identical to the value we determined using the Rey et al. (2004) data.

3. Pollution models

3.1. Construction of the models

As noted by Bekki & Norris (2006), the amount of helium required to form a later generation of helium rich bMS stars is far greater than would be produced by massive stars in the rMS population, unless the initial mass function was top-heavy. The large amount of helium could have come from the ejecta of a much larger stellar population, perhaps an ancient host galaxy of which the current ω Centauri is the remaining nucleus; this was the scenario advanced by Bekki & Norris (2006). Alternatively the helium could be the end product of an initial Population III population as advanced by Choi & Yi (2007).

An alternative scenario, which we admit is somewhat contrived, is that helium-rich material was accreted onto pre-existing rMS or MintP stars; the latter have $[\mathrm{M/H}] = -1.27$ but an ordinary helium abundance. Such stars will appear on the hot side of the rMS, as required by observation of the double main sequence, but the amount of helium required would be far less than in the case of bMS stars that are helium-rich throughout. As the helium-polluted stars ascend the giant branch, the deepening convection zone would erase the abundance gradient in these stars, and the final product would be expected to have TRGB total masses and core masses that are more like those of the rMS population.

The question of accretion onto globular cluster stars has been addressed in the past by Thoul et al. (2002). The mechanism for this is the classical Bondi accretion (Bondi 1952) in which the star, undergoing steady motion, accretes material in a spherically symmetric manner from an external medium. As shown by the Thoul et al. (2002) calculations, ω Centauri is not considered to be a good example of an environment likely to allow much accretion despite its deep gravitational well, though this may well have been different in the past especially if ω Centauri was originally part of a larger system as is often proposed. This pollution scenario has also been considered by Tsujimoto et al. (2007).

The starting models for the pollution scenario investigation were taken to be either the MintP or the rMS populations as shown in Table 1. We created a set of models with total fractional stellar mass accreted, composition and time delay from the ZAMS, with values shown in Table 3. The accreted material was of metal content $Z = 0.001$ so that the polluted stellar models always maintained the surface metallicity $[\mathrm{M/H}] = -1.27$ of the observed bMS population main sequence. These models ranged from $0.40 - 0.90 M_\odot$ in 0.05 $M_\odot$ increments. To each of these stars mass was accreted as a fraction of the total starting mass of the stellar model at a rate $10^{-10} M_\odot$ yr^{-1}, starting at a given age of the stellar model ranging from the ZAMS point (age of 0.0) up to a maximum of 9 Gyr in 3 Gyr increments. We chose our accretion rate based upon the calculations of Thoul et al. (2002) which show that for typical globular cluster environments the accretion rates expected are of the order $10^{-10} M_\odot$ yr^{-1}.

In Figure 7 we show the 13 Gyr main sequence isochrones for the rMS and bMS populations listed in Table 1. The accretion of helium-rich material will drag the rMS isochrone to the left and up in the $M_{\mathrm{bol}}, T_{\mathrm{eff}}$ plane. We also show the isochrone from a polluted rMS population scenario and how it overlaps the bMS isochrone at brighter magnitudes whilst merging with the rMS isochrone at fainter magnitudes. This behavior is described in more detail in Section 3.2 below.

Only certain combinations of the amount and helium fraction of the accreted material will shift isochrones to overlap the bMS. In Figure 8 we plot temperature shift produced by various amounts of accreted mass. The several curves display the shift as a function of the helium fraction (Y) of the accreted material. The horizontal axis is defined as the temperature difference between the bMS isochrone and that of the accreted population after a certain mass was added. It makes little difference if either rMS or MintP stars are the ones being polluted, since they start with similar masses and temperatures. The only allowed models are those that lie along $\Delta T = 0$. Only a very limited combination of parameters can provide the necessary shift of the isochrones required to produce the bMS population. The amount required is insensitive to the time at which the accretion takes place: later times increased ΔT by only $\sim$ 26K per 3 Gyr time increment. No amount of material with less than 45% helium would be adequate based upon extrapolation (we did not explore accretion with greater than 20% of the original starting mass). If the pollution occurred more recently than the ZAMS point, in the last few Gyr, then pollution with $\sim$ 35% helium would work.

In Table 4 we show the two of our pollution scenarios that produced the bMS population 13 Gyr isochrone, along with the TRGB mass and helium core mass of these models. In both of these scenarios the stars being polluted were rMS models. Results for the pollution of MintP models were very similar, requiring only slightly more mass in accreted material. The effects of polluting the stars of the rMS with the parameters do not appreciably affect the mass of the stars at the TRGB and that the mass of the helium core at the TRGB hardly changes. A ZAHB population generated with these stars as progenitors should be very similar to one created by regular rMS stars or MintP stars of normal helium content.

In Figure 9 we show the ZAHBs produced by polluted rMS and polluted MintP stars as well as those of the rMS, MintP and bMS stars. We also show, as thicker lines, the mass loss we inferred for the rMS stars from the CMD of ω Centauri, the same mass loss applied to the MintP and the polluted rMS and polluted MintP models as well as the equivalent mass loss of the bMS stars. The polluted-rMS HB is very similar to that of the rMS HB itself with the stars populating a similar range of color and only some 0.25 magnitudes more luminous (vs. 0.8 magnitudes for helium-rich homogeneous bMS stars) due to a combination of the slight metallicity enhancement and helium enhancement due to the pollution. A similar result is seen for the MintP and polluted MintP HB though with the stars being shifted in color to the red compared to the rMS stars by some 0.3 magnitudes in $B-V$. We find that these polluted stellar models when ascending the giant branches develop deep outer convective zones which result in the material accreted earlier being mixed with the original stellar material and thus being diluted by a factor of ~ 5. Therefore, the metallicity and helium content at the TRGB will be close to that of the original unpolluted star as seen in Table 4, where we list the ZAHB parameters for the polluted scenarios which can be contrasted with the parameters for the parent stars listed in Table 1. Thus the polluted star descendants will arrive on the ZAHB in a similar location on the CMD for a given mass loss, to be contrasted with the results derived earlier for bMS stars born with a homogeneous high level of helium.

Using the data in Table 4, we calculated the amount of helium required to pollute the rMS stars to the required level as compared to the amount of helium these stars would contain if their helium levels were homogeneous as for the bMS stars. Taking a typical $0.6M_{\odot}$ main sequence star, we see that the mass of helium in the accreting material varies from $0.022 - 0.034M_{\odot}$ depending upon the helium content of the polluting material. Now this same star if fully made up of helium rich material ($Y = 0.38$) would contain some $0.228M_{\odot}$ of helium. We find that the polluted stars require approximately $0.1 - 0.15$ times the amount of helium compared to the homogeneous high helium content stars.

We calculated the amount of helium that can be produced from the rMS stars that have already ended their lives, assuming such a population directly produced the observed bMS population. We assumed a total stellar mass of 5×10^6 solar masses for ω Centauri today. We took yield calculations from the literature (Portinari et al. 1998; Van den Hoek & Groenewegen 1997; Ventura & D'Antona 2005). Using a variety of IMF's including the Salpeter IMF

(Salpeter 1955), the Miller-Scalo IMF (Miller & Scalo 1979), the Kroupa-Tout-Gilmore IMF (Kroupa et al. 1993), the Scalo IMF (Scalo 1998) and the Kroupa IMF (Kroupa 2001) we calculated the mass of helium produced and ejected back into the cluster environment assuming none was lost from the cluster. We took account of the evolutionary lifetimes of the rMS and bMS stars as represented by the different RGB tip masses at our assumed age of ω Centauri of 13 Gyrs. This allowed us to calculate the mass of the original rMS and bMS populations at their formation from the current observed number fractions of these populations. We also calculated the mass of helium required to create the bMS as a primordial helium rich population. Our results are shown in Table 5. We note that Tsujimoto et al. (2007) perform a similar calculation for the Salpeter IMF and show results similar to ours.

We find that, depending upon the IMF chosen, that no more than 25% of the helium required to make a helium rich bMS population can be produced from the intermediate mass AGB stars ($3-8$ solar masses) of the rMS population. For the Kroupa-Tout-Gilmore IMF this number is about 1%. Even if all the stars above the current RGB tip mass are included in the calculation the mass of helium is still only from $20\% - 75\%$ of that required and this material would be of a far lower helium fraction than that incorporated in the proposed levels for the bMS stars. We thus find it implausible that the bMS population can be born from the helium rich AGB ejecta of the rMS population.

We note that the pollution scenarios require only some $10\% - 15\%$ of helium compared to the homogeneous bMS stars. Such helium amounts are within the bounds of all but the aforementioned Kroupa-Tout-Gilmore IMF choice. The calculations above do not vary appreciably for alternative yields in the literature for helium production. Karakas et al. (2006) point out that another problem for the rMS AGB stars to have formed the bMS stars is that for AGB helium yields of the necessary magnitude ($Y > 0.3$) the total C+N+O levels would be increased enormously. This is inconsistent with the observed constant values of the C+N+O abundances.

3.2. Observational consequences of pollution models

An interesting difference between the polluted model isochrone and our theoretical bMS isochrone is shown in Figure 7. Both sets of models exhibit a gradual merging with the rMS isochrone but at a significantly different bolometric luminosity. It is seen in Villanova et al. (2007) that the observed bMS and rMS sequences appear to merge at magnitude of $R \sim 21.3$. We find with our models that this merging corresponds to a $M_{\rm bol} \sim 7.69$ for bMS stars with a mass of $0.410 M_{\odot}$ and $M_{\rm bol} \sim 7.65$ for rMS stars with a mass of $0.495 M_{\odot}$. However, we find that our bMS and rMS isochrones do not merge until $M_{\rm bol} \sim 8.8$ some 1.1 magnitudes fainter than is observed. In contrast our pollution scenario 2 from Table 4 merges with the rMS isochrone at $M_{\rm bol} \sim 7.5$. We note that the luminosity at which the merging takes place with stellar models of $0.45 M_\odot$ or less is sensitive primarily to the choice of the equation of state employed in the stellar model calculations. Sollima et al. (2007) showed theoretical models calculated using the evolution code of Straniero et al. (1997) using a different equation of state than ours and that their bMS and rMS sequences merged close to the observed merge point. We also tested our models with the old Yale equation of state and found that the merging did not occur until $M_{\rm bol} \sim 10$.

Using our theoretical models we calculated the expected $(B-R)/(B+V+R)$ statistic for a composite population of the bMS (30%), rMS (65%) and the known metal rich population ([M/H] ~ -0.6) numbering some 5% of the stars. We calculated this statistic for three mean mass losses for the rMS population and for bMS stars coeval, 2 Gyr and 4 Gyr younger than the majority rMS population. We repeated this for polluted rMS models representing the bMS stars fraction of the composite population. The results of this are plotted in Figure 10 where the labeled cases (A thru F) are described in Table 5. Using the observed CMD, we calculated the ω Centauri $(B-R)/(B+V+R)$ statistic to be 0.85 ± 0.01. We predict various age differences for the rMS and bMS populations that both depend on the helium content and mass loss. These age differences are shown in Table 6. We can see immediately that for a given mass loss and $(B-R)/(B+V+R)$ statistic value that the age differences for the composite population containing bMS stars implies a much larger age difference than if the bMS stars are replaced by polluted rMS stars.

The constraint on the age difference between the various populations of ω Centauri has been previously investigated. Using the morphology of the turn-off region Sollima et al. (2005) put a maximum on the age difference between the rMS and bMS stars (irrespective of helium enhancement) of $\sim$ 1.5 Gyr. In their main sequence fitting of model isochrones Lee et al. (2005) determined that the age difference between the rMS and bMS stars was $\sim$ 1 Gyr. We can see from the data in Table 5 that our models predict that only mean mass losses in the 0.2M$_\odot$ range with polluted rMS stars reproduce a $(B-R)/(B+V+R)$ statistic in line with observation. All the scenarios with the high helium bMS stars imply age differences that are much too large. Furthermore, we earlier calculated the mass loss range from the ω Centauri CMD using the prominent HB clump as representing the majority rMS population and obtained mass losses in the range $0.168 - 0.247 M_\odot$, such mass losses are within or close to the allowable range based upon figure 10.

4. Summary

It has been hypothesized that the double main sequence of ω Centauri reveals an intermediate metal-poor population that have a large enhancement of helium, contrary to expectation of standard stellar theory. This hypothesis seemed even more credible after spectroscopic analysis confirmed that the blue main sequence stars were indeed more metal-rich than the majority red main sequence. The proposed helium levels in these stars are extremely large compared to known stellar populations, imply an extremely large and preferential enrichment history for their formation whilst coexisting with, or forming from, a majority stellar population that is not unusual in any noticeable way.

We confirmed using our latest YREC stellar models that the proposed helium rich bMS stars do lie to the blue side of the more metal-poor rMS stars. We developed a new procedure to allow mass loss comparison between stars of different TRGB masses so as to predict their HB morphology and compare to the observations. Under the assumption that the large clump of the ω Centauri HB is a product of the majority rMS metal-poor population, we inferred that the mass loss suffered by these stars on the RGB spans a range of $0.168 - 0.247 M_{\odot}$ from TRGB progenitors of $0.814 M_{\odot}$ at an age of 13 Gyrs. This in turn implied that the proposed high helium bMS stars would have lost a minimum of $0.102 - 0.147 M_{\odot}$ from a TRGB progenitor of some $0.629 M_{\odot}$ at the same age. We find such helium rich stars would appear on the HB in the blue tail below the majority clump that is assumed to be from the rMS stars. If we assume all such stars on the CMD of the ω Centauri HB are attributable to the bMS population then we have only $\sim 25\%$ of the bMS plus rMS stars residing there. This seems distinctly at odds with the $\sim 37\%$ of bMS plus rMS star total we observe in the MS itself. We also note that if we use our Case II or Case III mass losses for these stars the HB bMS stars should appear far down the blue tail in a large clump clearly separated from the observed majority clump we identify with the rMS stars. Such a disconnected clump at the bottom of the blue tail of the ω Centauri HB is not seen at all.

Unless the mass loss mechanism for the proposed high helium bMS stars operates differently from the rMS stars causing them the reside in the large observed clump then these stars are absent from the HB of ω Centauri. In fact, for the bMS stars to be hiding amongst the majority HB clump then their mass loss must be in the range $0.059 - 0.101 M_{\odot}$, where the lower limit is determined by the fact we do not see overluminous HB stars in substantial numbers above the main HB clump. Prior observations of the instability strip RR Lyrae variables have not found evidence of high helium stars there, implying that the mass loss of these stars on the RGB was not far lower than what we have assumed. We noted earlier that if the bMS stars were $2 - 5$ Gyr younger they would also appear in the instability strip of ω Centauri but such age differences have been ruled out by turn-off morphology in other studies.

It is possible to create a blue main sequence theoretically by the pollution of existing rMS or MintP stars with helium rich material for limited combinations of helium content and mass accreted. The helium content of such material is not far from the range of the latest intermediate mass AGB stellar yields (Herwig 2004), especially if the accretion is relatively recent. The total mass of the accreted material is in line with estimates of the possible pollution in a globular cluster environment (Thoul et al. 2002). We do note that the AGB helium yields we require are on the upper end (or slightly beyond) of such calculations and that the mass accreted to create our blue main sequences is incompatible with the current ω Centauri environment, though possibly not that of past when the cluster was not only more massive but the velocity dispersion lower; both of which would increase the amount of accretion possible onto existing stars. Creating bMS stars out of homogeneous helium rich material is not the only possible mechanism for their formation, and pollution via accretion of AGB ejecta in a globular cluster environment is another possibility. We see that of the observed ω Centauri RR Lyrae variables the presence of both MintP stars and rMS stars but no helium-rich bMS stars, this implies that at least some MintP stars formed with normal helium enrichments. An accretion pollution scenario has also been hypothesized in the past by Cannon et al. (1998) in regard to the main sequence abundance anomalies in the globular cluster 47 Tuc, where the C and N abundance variations are seen on the main sequence and in red giants. We note our simple pollution scenario does not explain the abundance variations seen on both the main sequence and giant branches, as they would be washed out as the stars evolve up the RGB.

The polluted star scenario predicts that the ZAHB for such a population should not differ appreciably from that of the unpolluted parent stars. We see from this that we would observe in the ω Centauri CMD a double main sequence and a HB that possesses a majority single clump, very few over luminous stars in the horizontal region of the HB, no large disconnected clump of stars in the HB blue tail and no RR Lyrae variables that are over luminous. This is what is observed in contrast to the predictions of the homogeneously helium rich bMS stars that have been proposed. The polluted star scenario though requiring certain combinations of pollution helium content and total mass accreted does not require the very large helium amounts that the proposed bMS stars do, amounts that seem greater than that possible from ejecta of more massive rMS stars in ω Centauri.

Another prediction from our modeling is that the polluted stars will merge with the rMS stars at approximately the observed luminosity whereas our model homogeneous bMS stars do not do this until about 1.1 magnitudes fainter. The position of the this merger may turn out to be an important diagnostic in determining the composition of the bMS stars.

We used the $(B-R)/(B+V+R)$ statistic that is usually applied to the investigation of single stellar population horizontal branches in globular clusters. When we apply our calculated $(B-R)/(B+V+R)$ of 0.85 ± 0.01 for ω Centauri to theoretical predictions of this statistic using our models we found that the high helium bMS star models predict age differences for the bMS population that are too great when compared to turn-off morphology estimates. The pollution scenario for mass losses less than $\sim 0.2 M_{\odot}$ are within the allowable limit of age differences. A result that is also approximately the range of estimated mass losses for the rMS population $(0.168 - 0.247 M_{\odot})$ we inferred from the ω Centauri CMD using our theoretical models.

We would like to thank M. Pinsonneault and D. Weinberg for helpful suggestions and A. Sollima for kindly furnishing to us the HST data. We would also like to thank the anonymous referee whose many and detailed comments have greatly improved this paper.

REFERENCES

Alexander, D. R., & Ferguson, J. W., 1994, ApJ, 437, 879

Allard, F., & Hauschildt, P. H. 1995, ApJ, 445, 433

An, D., Terndrup, D. M., Pinsonneault, M. H., Paulson, D. B., Hanson, R. B., & Stauffer, J. R., 2007, ApJ, 655, 233

Bahcall, J. N., & Loeb, A., 1990, ApJ, 360, 267

Bahcall, J. N., Pinsonneault, M. H., & Basu, S., 2001, ApJ, 555, 990

Bedin L., Piotto G., Anderson J., Cassisi S., King I., Momany Y., & Carraro G., 2004, ApJ, 605, L125

Bekki, K., & Norris, J., 2006, ApJ, 637L, 109

Bergbusch, P. A., & Vandenberg D. A., 1992, ApJS, 81, 163

Böhm-Vitense, E. 1958, Z. Astrophys., 46, 108

Bondi, H., 1952, MNRAS, 112, 195

Bono, G., Balbi, A., Cassisi, S., Vittorio, N., & Buonanno, R. 2002, ApJ, 568, 463

Bono, G., Caputo, F., & Marconi, M. 1995, AJ, 110, 2365

Cannon, R. D., Croke, B. F. W., Bell, R. A., Hesser, J. E., & Stathakis, R. A., 1998, MNRAS, 298, 601

Catelan, M., 2000, ApJ, 531, 826

Choi, E., & Yi, S. K., MNRAS, 375, L1

Cox, J. P., & Guili, R. T., 1968, Principles of Stellar Structure (New York: Gordon and Breach)

D'Antona, F., Caloi, V., Montalban, J., Ventura, P., & Gratton, R., 2002, A&A, 395, 69

D'Antona, F., Bellazzini, M., Caloi, V., Fusi-Pecci, F., Galleti, S., & Rood, R. T., 2005, ApJ, 631, 868

D'Cruz et al., 2000, ApJ, 530, 352

Delahaye, F., & Pinsonneault, M., 2005, ApJ, 625, 563

Dickens, R. J., & Wooley S. J., 1967, Royal Obs. Bull., 128, E255

Ferraro, F. R., Sollima, A., Pancino, E., Bellazzini, M., Origlia, L., Straniero, O., & Cool, A., 2004, ApJ, 603, L81

Freeman, K. C., & Rodgers, A. W., 1975, ApJ, 201, L71

Fukugita, M., & Kawasaki, M. 2006, ApJ, 646, 691

Green, E. M., Demarque, P., & King, C. R., 1987, the Revised Yale Isochrones and Luminosity Functions (New Haven: Yale Univ. Obs.)

Grevesse, N., & Noels, A., 1993, in Origin and Evolution of the Elements, ed. N. Prantzos, E. Vangioni-Flam, & M. Cass (Cambridge: Cambridge Univ. Press), 15

Gruzinov, A., & Bahcall, J., 1998, ApJ, 504, 996

Guenther, D. B., Demarque, P., Kim, Y.-C., & Pinsonneault, M. H., 1992, ApJ, 387, 372

Herwig, F., 2004, ApJS, 155, 651

Iglesias, C. A., & Rogers, F. J., 1996, ApJ, 464, 943

Itoh, N., Hayashi, H., & Nishikawa, A., 1996, ApJS, 102, 411

Jimenez, R., Flynn, C., MacDonald, J., & Gibson, B. K., 2003, Science, 299, 1552

Karakas, A., Fenner, Y., Sills, A., Campbell, S. W., & Lattanzio, J. C., 2006, preprint (astro-ph/0608366)

Kroupa, P., Tout, C. A., & Gilmore, G., 1993, MNRAS, 262, 545

Kroupa, P., 2001, MNRAS, 322, 231

Lee Y.-W., Demarque P., & Zinn R., 1994, ApJ, 423, 248

Lee Y.-W., Joo S-J., Han S-I., Chung C., Ree C., Sohn Y-J., Kim Y-C., Yoon S-J., Yi S. & Demarque P., 2005, ApJ621, L57

Maeder, A., & Meynet, G., 2006, A&A, 448, L37

Miller G. E., & Scalo, J. M., 1979, ApJS, 41, 513

Momany, Y., Bedin, L. R., Cassisi, S., Piotto, G., Ortolani, S., Recio Blanco, A., De Angeli, F., & Castelli, F., 2004, A&A, 420, 605

Norris, J. E., 2004, ApJ, 612, L25

Norris, J., & De Costa G. S., 1995, ApJ, 447, 680

Norris, J. E., Freeman, K. C., & Mighell, K. J., 1996, ApJ, 462, 241

Olive, K. A., & Skillman, E. D. 2004, ApJ, 617, 29

Origlia, L., Ferraro, F. R., Fusi Pecci, F., & Rood, R. T., 2002, ApJ, 571, 458

Pagel, B. E. J., 1992, IAU Symp. 149, Stellar Populations in Galaxies, ed. B. Barbury, & A. Renzini, (Dordrecht: Kluwer), 133

Pancino E., Ferraro F., Bellazzini M., Piotto G., & Zoccali M., 2000, ApJ, 534, L83

Pinsonneault, M. H., Terndrup, D. M., Hanson, R. B., & Stauffer, J. R., 2003, ApJ, 598, 588

Piotto et al., 2005, ApJ, 621, 777

Portinari, L., Chiosi, C., & Bressan, A., 1998, A&A, 334, 505

Rey, S.-C., Lee, Y.-W., Ree, C.-H., Joo, J.-M., & Sohn Y.-J., 2004, AJ, 127, 958

Rogers, F. J., Swenson, F. J., & Iglesias, C. A., 1996, ApJ, 456, 902

Salpeter, E., 1955, ApJ, 121, 161

Scalo, J., 1998, in ASP Conf. Ser., 142, The Stellar Initial Mass Function, 201

Saumon, D., Chabrier, G., & Van Horn, H. M., 1995, ApJS, 99, 713

Serenelli, A., & Weiss, A. 2005, A&A, 442, 1041

Sills, A., Pinsonneault, M. H., & Terndrup, D. M., 2000, ApJ, 534, 335

Sollima, A., Ferraro, F. R., Bellazzini, M., Origlia, L., Straniero, O., & Pancino, E., 2007, ApJ, 654, 915

Sollima, A., Borrisova, J., Catelan, M., Smith, H. A., Minniti, D., Cacciari, C., & Ferraro, F. R., 2006, ApJ, 640, L43

Sollima, A., Pancino, E., Ferraro, F., Bellazzini, M., Straneiro, O., & Pasquini, L., 2005, ApJ, 634, 332

Straniero, O., Chieffi, A. & Limongi, M., 1997, ApJ, 490, 425

Suntzeff, N. B., & Kraft, R. P., 1996, AJ, 111, 1913

Thoul, A. A., Bahcall, J. N., & Loeb, A., 1994, ApJ, 421, 828

Thoul, A., Jorissen, A., Goriely, S., Jehin, E., Magain, P., Noels, A., & Parmantier, G., 2002, A&A, 383, 491

Thuan, T. X., & Izotov, Y. I. 2002, Space Sci. Rev., 100, 263

Tsujimoto, T., Shigeyama, T., & Suda, T., 2007, ApJ, 654, L139

VandenBerg, D. A., & Clem, J. L., 2003, AJ, 126, 778

Van den Hoek, L. B., & Groenewegen, M. A. T., 1997, A&AS, 123, 305

Ventura, P., & D'Antona, F., 2005, A&A, 439, 1075

Villanova, S., Piotto, G., King, I. R., Anderson, J., Bedin, L. R., Gratton, R. G., Cassisi, S., Momany, Y., Bellini, A., Cool, A. M., Recio-Blanco, A. & Renzini, A., 2007, preprint (astro-ph/0703208)

Weiss, A., Salaris, M., Ferguson, J. W., & Alexander, D. R., 2006, preprint (astro-ph/0605666)

Yi, S., Kim, Y.-C., & Demarque P., 2003, ApJS, 144, 259

This preprint was prepared with the AAS LaTeX macros v5.2.

Table 1. Model population parameters.

Parameter	rMS	bMS	MintP
Z	0.0005	0.001	0.001
Y	0.231	0.382	0.232
[M/H]	–1.57	–1.27	–1.27
TRGB mass ($M_{\odot}$)	0.814	0.629	0.826
TRGB core mass ($M_{\odot}$)	0.485	0.455	0.479

Table 2. Mass loss for the bMS population ($M_\odot$).

	bMS mass loss		
rMS Mass loss	Case I	Case II	Case III
0.12	0.072	0.084	0.114
0.16	0.097	0.112	0.152
0.20	0.118	0.140	0.190
0.24	0.143	0.168	0.228
0.28	0.168	0.196	0.266

Table 3. Pollution scenario parameter matrix.

Population	Fractional Mass	X	Y	Z	Accretion Age (Gyr)
MintP	0.2	0.699	0.30	0.001	0.0
rMS	0.159	0.649	0.35		3.0
	0.129	0.599	0.40		6.0
	0.1	0.549	0.45		9.0
	0.07	0.499	0.50		
	0.04				

Table 4. Pollution scenarios and their calculated ZAHB properties.

Population	Fractional Mass	Z	Y	TRGB Mass ($M_\odot$)	Helium Core Mass ($M_\odot$)
Scenario 1	0.07	0.001	0.5	0.810	0.481
Scenario 2	0.129	0.001	0.45	0.811	0.481
Polluted rMS ZAHB	-	0.0006	0.276	-	0.481
Polluted MintP ZAHB	-	0.001	0.276	-	0.481

Table 5. Helium Yield Calculations for different IMF's

IMF	Helium required ($M_\odot$)	Helium produced (all stars)($M_\odot$)	Helium produced (AGB stars only)($M_\odot$)
Salpeter	5.1×10^5	2.3×10^5	5.9×10^4
Miller-Scalo	1.0×10^6	6.8×10^5	2.5×10^5
Scalo	7.0×10^5	4.0×10^5	1.1×10^5
Kroupa-Tout-Gilmore	4.3×10^5	8.6×10^4	4.0×10^3
Kroupa	8.8×10^5	6.5×10^5	1.6×10^5

Table 6. Calculated age differences.

Case	Mean rMS mass loss ($M_\odot$)	Helium enhancement	Age difference (Gyrs)
A	0.20	Homogeneous	-1.55 - -1.75
B	0.24	Homogeneous	-3.35 - -3.80
C	0.28	Homogeneous	-5.55 - -6.15
D	0.20	Polluted	-0.65 - -0.75
E	0.24	Polluted	-2.15 - -2.25
F	0.28	Polluted	-2.45 - -2.55

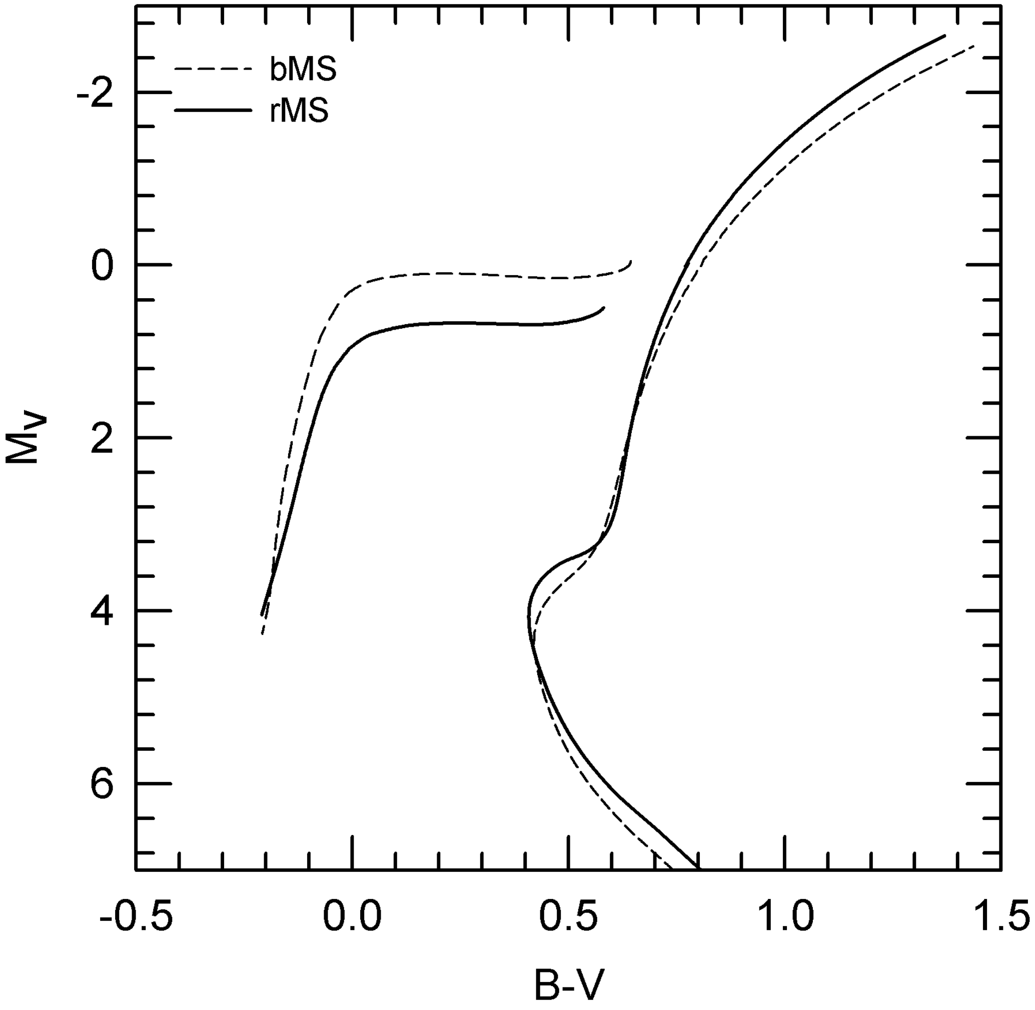

Fig. 1.— The rMS and bMS 13 Gyr isochrones using the parameters in Table 1.

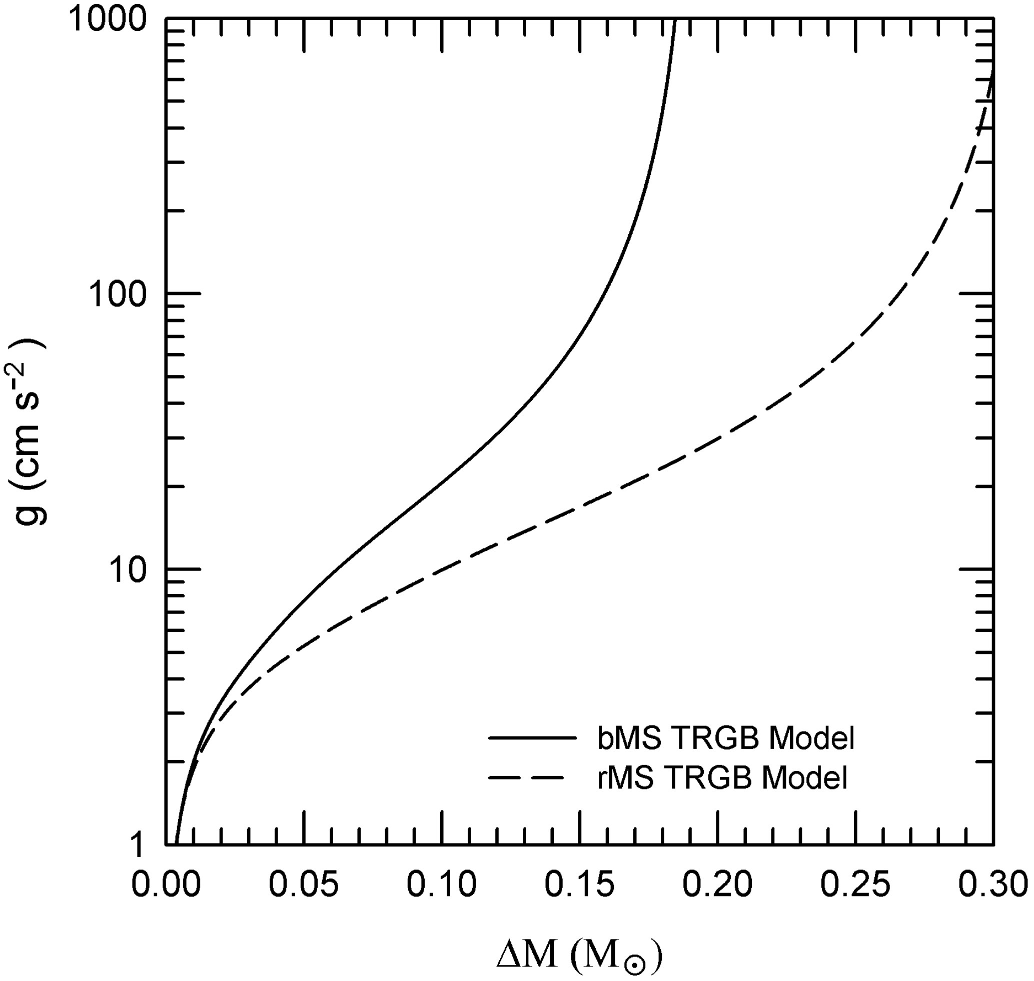

Fig. 2.— Stratification of the rMS and bMS models near the TRGB. The plot shows the gravitational acceleration as a function of stellar mass below the surface.

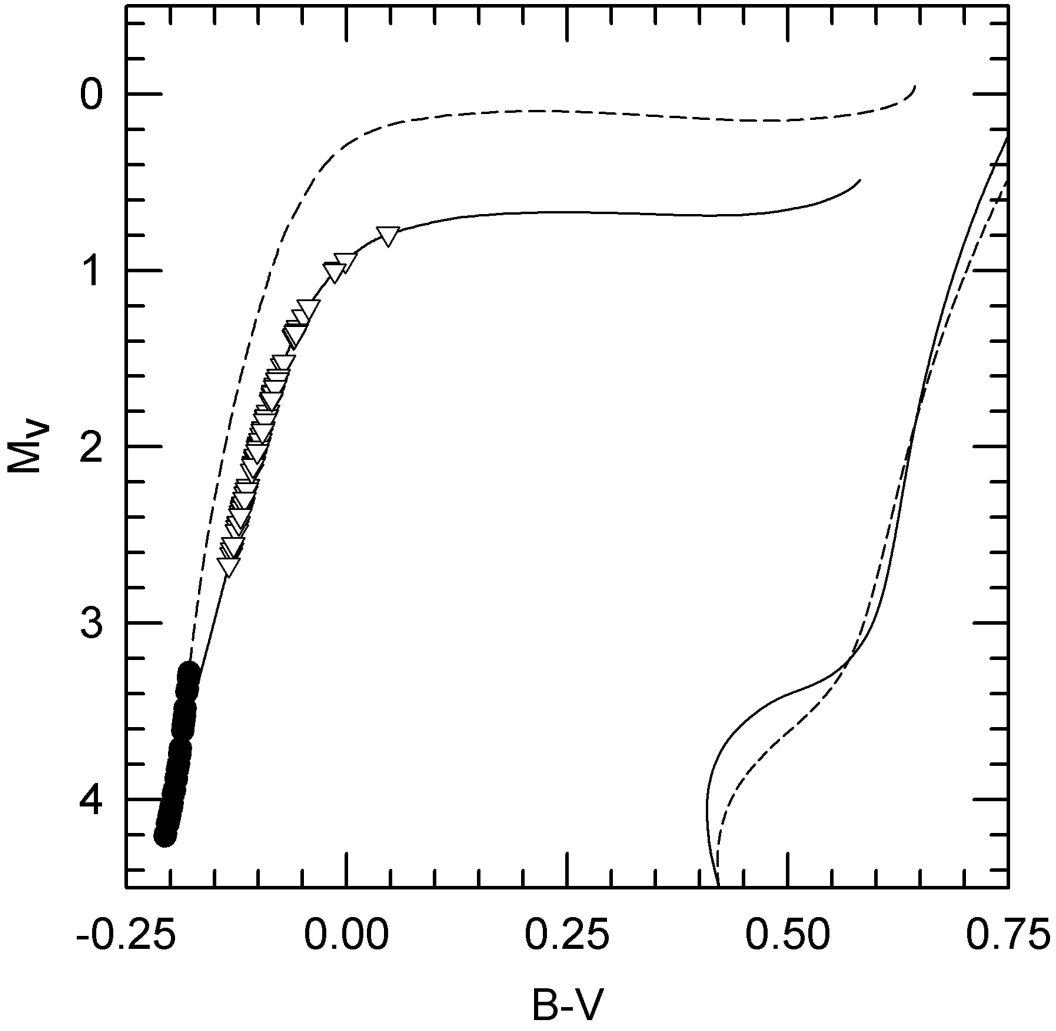

Fig. 3.— rMS (open triangles) and bMS (filled circles) 13 Gyr ZAHBs populated for a rMS mean mass loss of $0.24 M_{\odot}$ and a bMS mean mass loss of $0.143 M_{\odot}$ using Case I mass losses.

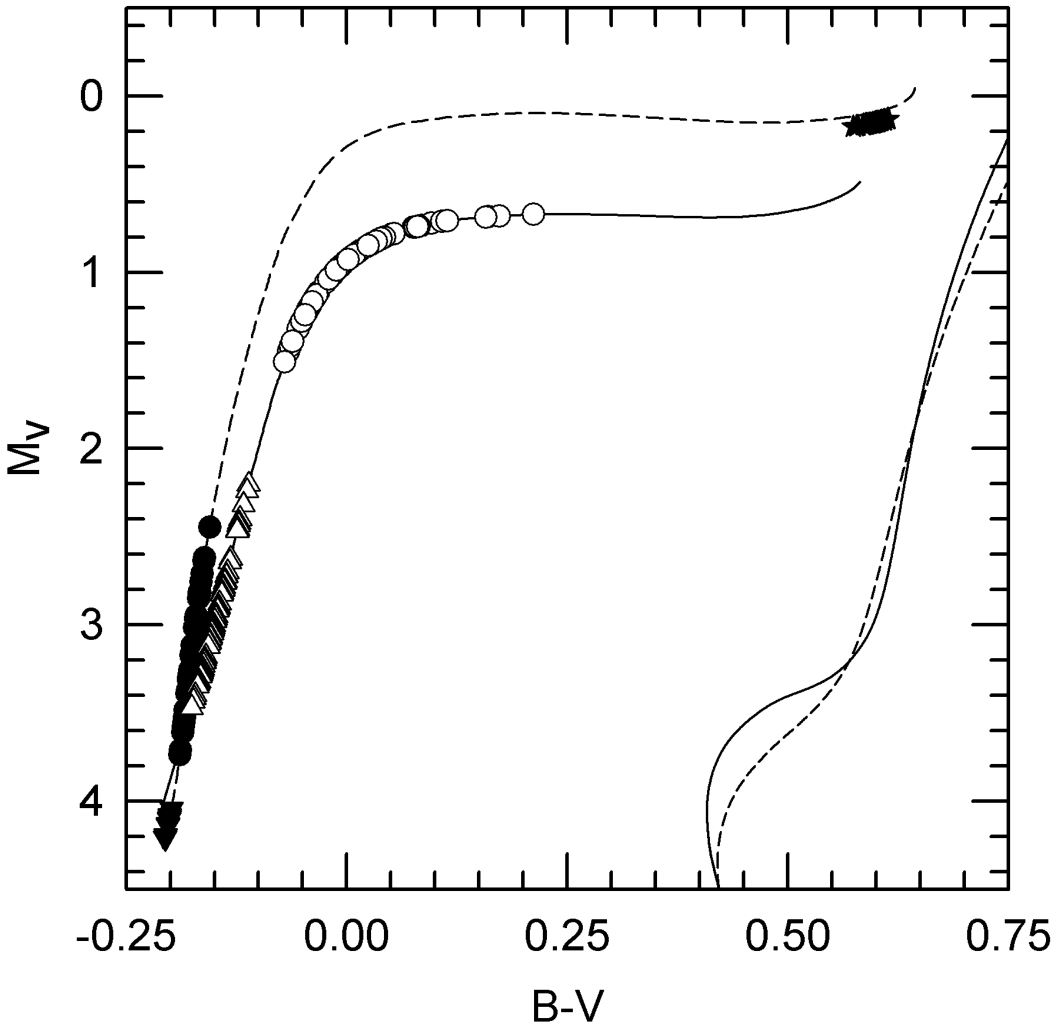

Fig. 4.— The rMS 13 Gyr ZAHBs populated for rMS mean mass losses of $0.20 M_\odot$ (open circles) and $0.28\ M_\odot$ (open triangles) and the bMS 13 Gyr population populated for bMS mean mass losses of $0.118\ M_\odot$ (filled circles) and $0.168\ M_\odot$ (filled triangles) and the bMS 7 Gyr population with mean mass loss $0.143 M_\odot$ (filled stars). All bMS mass losses are using Case I.

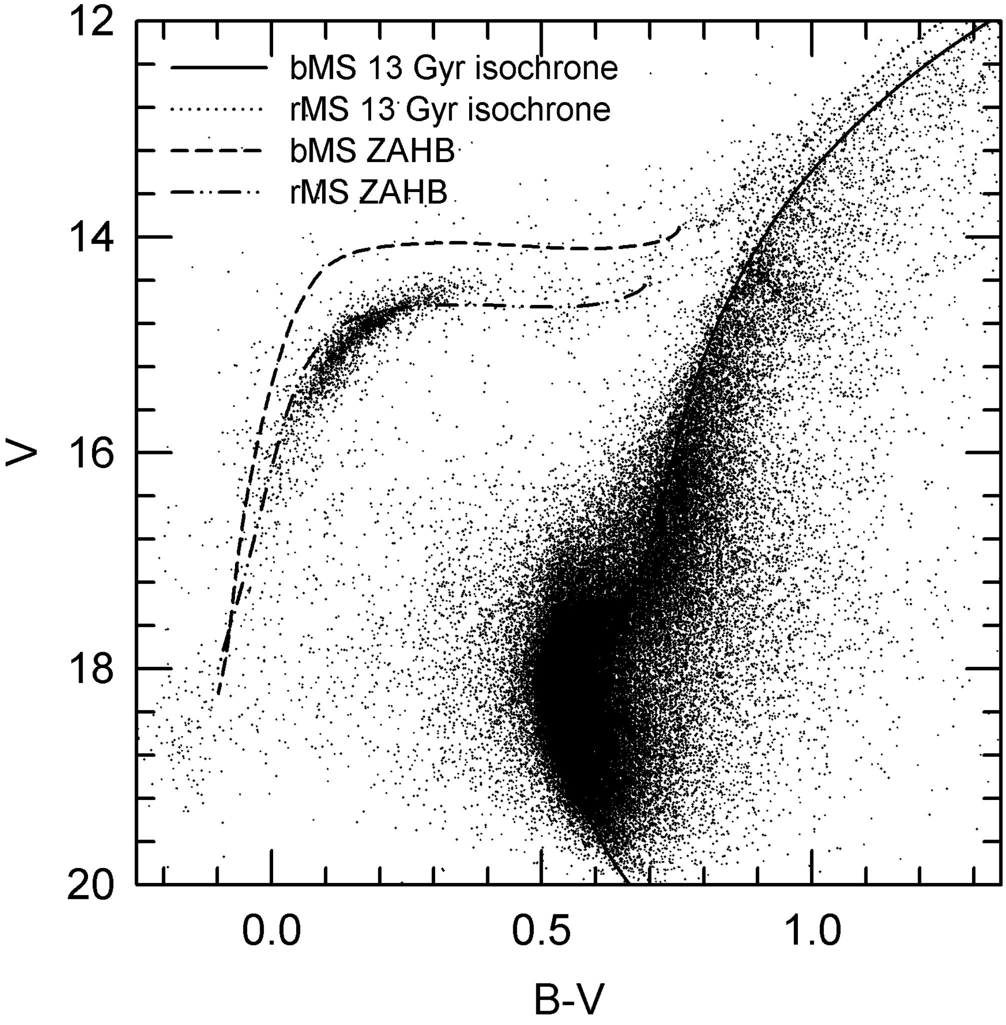

Fig. 5.— CMD of ω Centauri with 13 Gyr rMS and bMS isochrones. Photometry is from Rey et al. (2004).

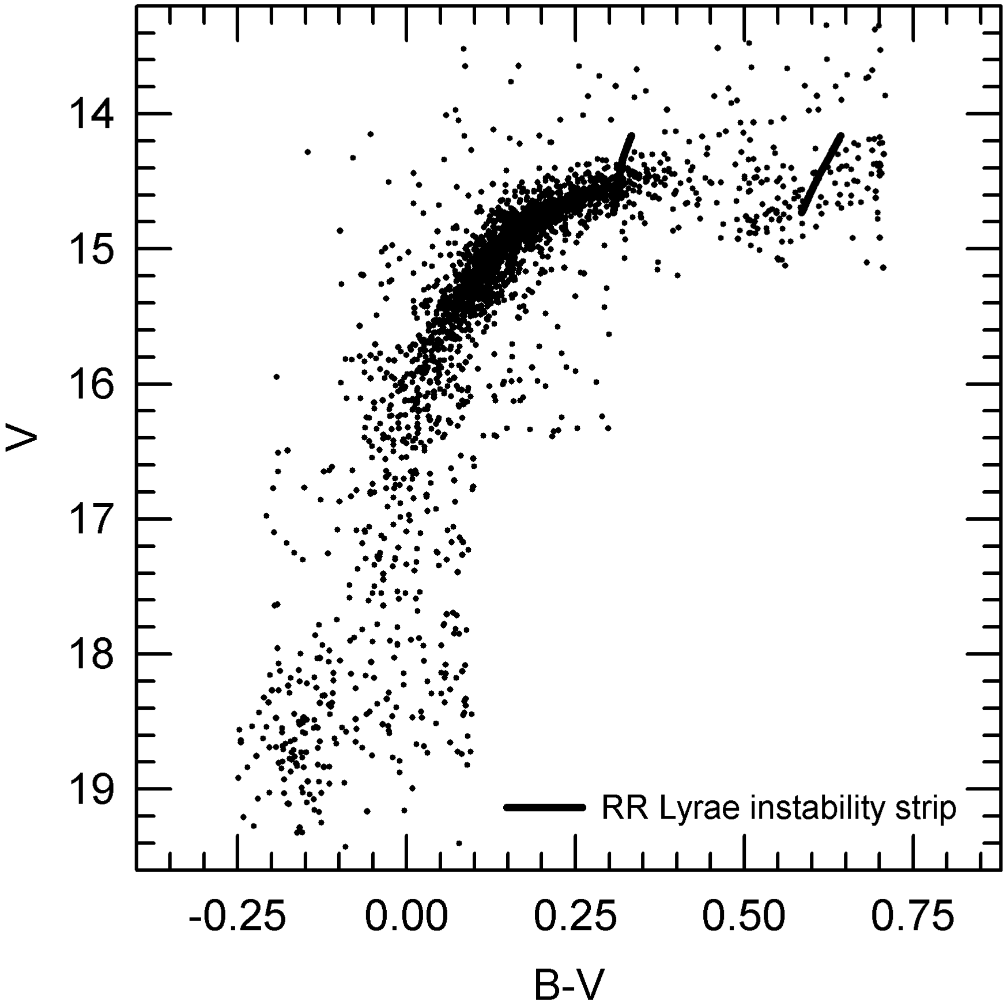

Fig. 6.— Horizontal branch CMD of ω Centauri showing the RR Lyrae instability strip for the rMS population.

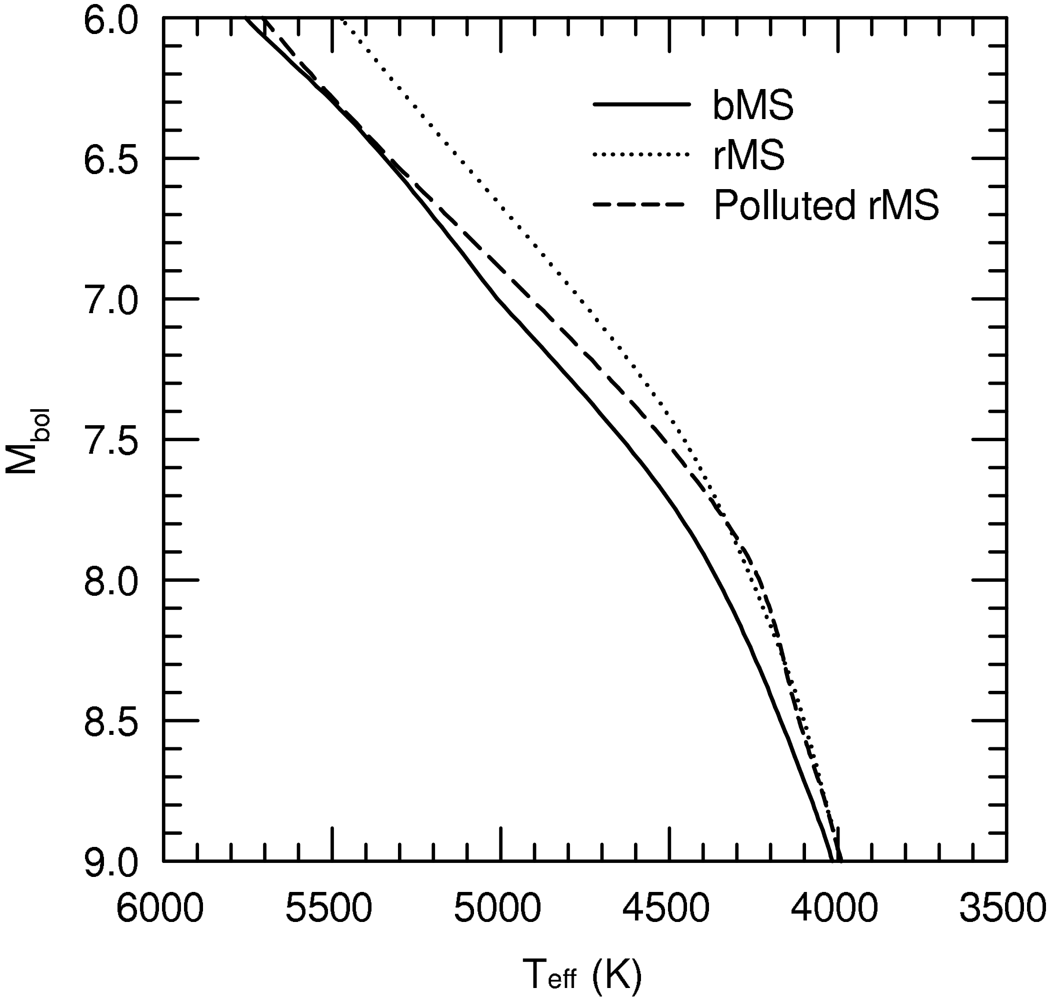

Fig. 7.— Model main sequences of the rMS and bMS populations and a polluted rMS sequence.

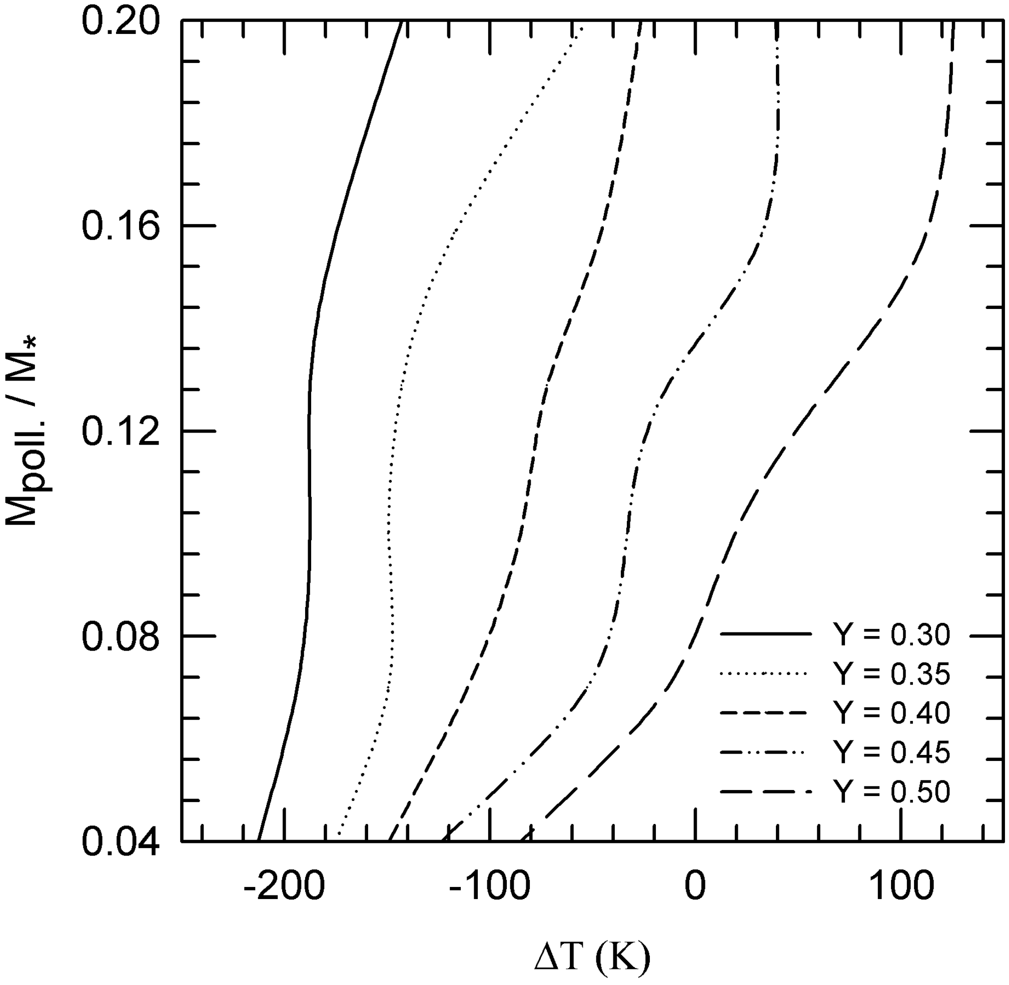

Fig. 8.— Mass fraction of pollution to total stellar mass vs. change in $T_{\rm eff}$ (ΔT) for rMS stellar models.

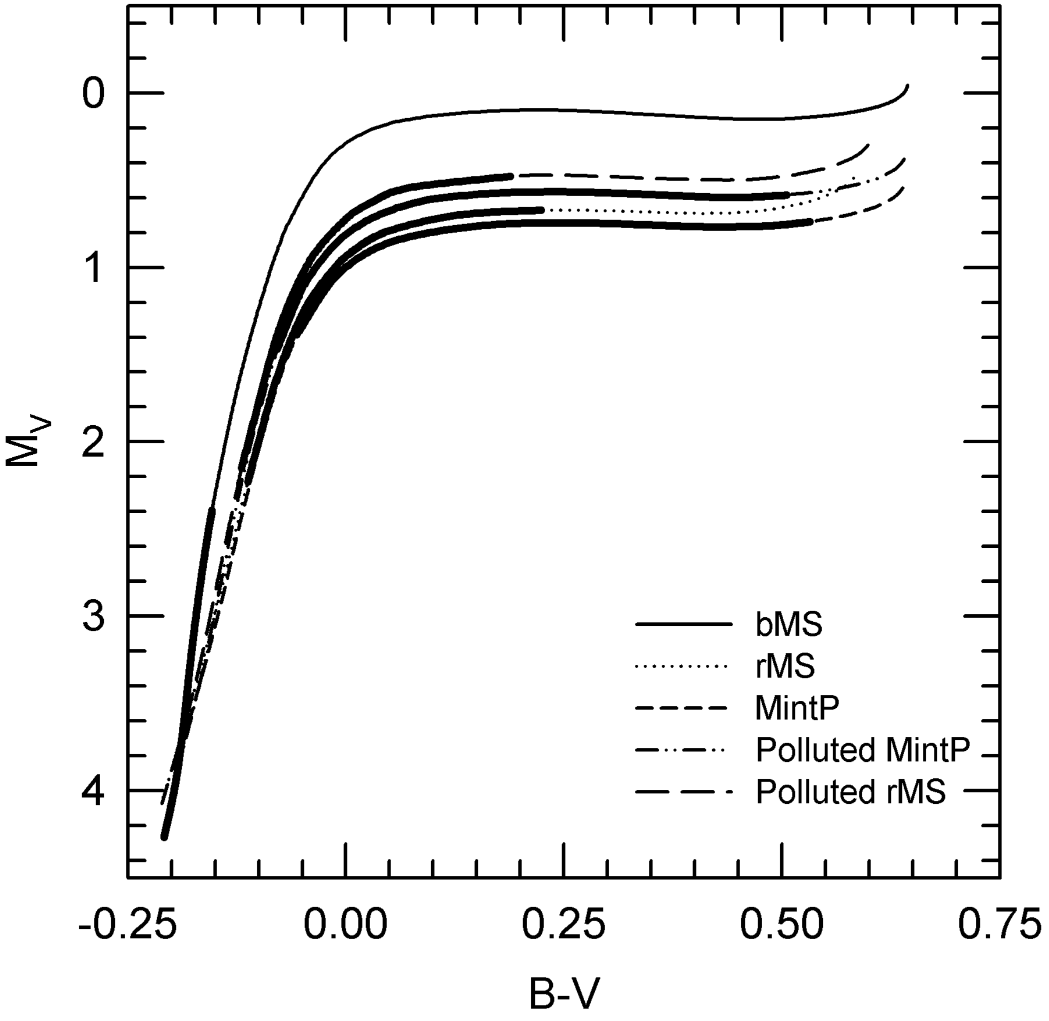

Fig. 9.— Standard and pollute population ZAHB's and equivalent mass losses (Case I) based upon the inferred rMS mass loss of $0.168M_{\odot} - 0.247M_{\odot}$

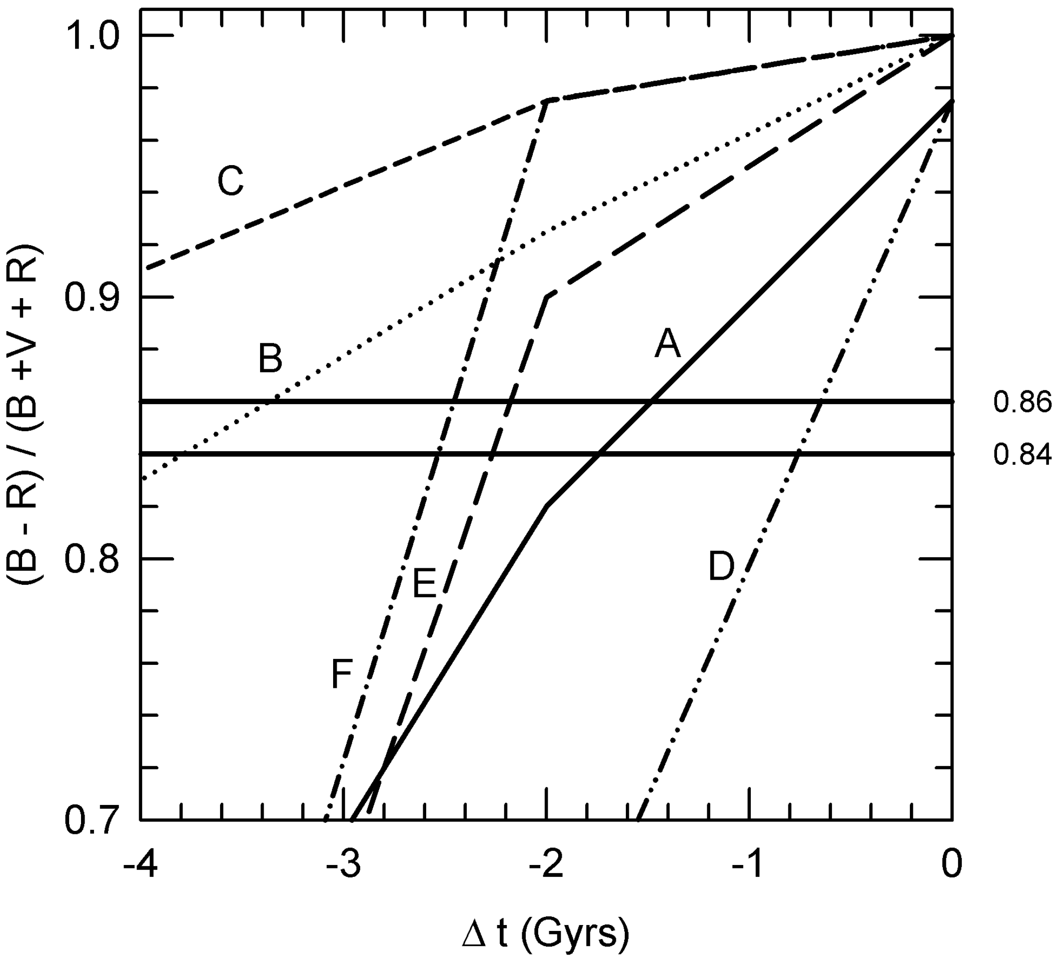

Fig. 10.— $(B - R)/(B + V + R)$ statistic vs. age difference of a composite ω Centauri population. See Table 6 for the case (A - F) details.